Article

Not peer-reviewed version

Series Resonant LED Driver with Current Equalization Based on the Differential-Mode Transformer

Kuo-Ing Hwu * and Jun-Yi Lee

Posted Date: 28 April 2025

doi: 10.20944/preprints202504.2363.v1

Keywords: Series Resonant Converter; LED Driver; Differential-mode transformer; Current Equalization and LED String Expansion

 doi:10.20944/preprints202504.2363.v1

Article

Series Resonant LED Driver with Current Equalization Based on the Differential-Mode Transformer

Kuo-Ing Hwu * and Jun-Yi Lee

Department of Electrical Engineering, National Taipei University of Technology, 1, Sec. 3, Zhongxiao E. Rd. Taipei 10608, Taiwan

* Correspondence: eaglehwu@ntut.edu.tw; Tel.: +886-2-27712171 (ext.2159)

Abstract: In this research, a series resonant LED driver circuit based on the differential-mode transformer for current equalization is proposed. In this circuit, the series resonant converter adopts controlled frequency modulation to change the energy transferred to the output while realizing zero voltage switching (ZVS) turn-on of the half-bridge switch. To deal with the problem of unequal LED currents caused by two different forward conduction voltages of the output LED strings, a differential-mode transformer is employed to balance the currents between the two LED strings and the relationship between the magnetizing inductance and the percentage of current sharing error is derived to facilitate the design. Furthermore, only the current of one LED string needs to be sensed to achieve current equalization, while the current of the other LED string is automatically determined by the differential-mode transformer.

Keywords: series resonant converter; LED driver; differential-mode transformer; current equalization and LED string expansion

1. Introduction

The invention of light emitting diodes (LEDs) and the advancement of power supplies have led to improving lighting systems, replacing the inconveniences of traditional lamps [1]. LED lighting is characterized by high luminous efficiency, long life and high reliability, but due to the low luminous flux of a single LED, it cannot be used in most applications, and when there is a high demand for illumination, such as street lighting, plaza lighting, and other applications, it is necessary to combine a few LEDs in series or in parallel. However, the V-I curve of each LED is not the same due to negative temperature coefficient, leading to a large change in the conduction current, so the LED driver is designed to a fixed current to power LED strings [2], and the current equalization control is required to solve the problem of current imbalance between the LED strings.

Up to now, there are many LED current equalization strategies have been proposed can be divided into two categories, namely, active current equalization and passive current equalization. For the active current equalization method, it can be divided into linear type and switching type. First of all, for the linear type, it uses the linear regulator or current mirror connected in series with the LED string. Generally speaking, the linear regulator is the switch is operated in the linear region and can be regarded as the variable resistor [3]. In order to achieve the LED current balance, the literature [4] proposes an adaptive voltage circuit between the main power stage and the LED strings, so that the voltage across the switch of the linear regulator can be regulated to reduce the loss of energy. Although it is simple to control the variable resistance to achieve current equalization, the power loss during conduction is large, so it is more suitable for use in low-power applications. As for current mirroring, it utilizes the characteristics of transistors to map the reference current to other transistors in equal or proportional currents so that the currents flowing through each transistor are equal. This active method commonly uses semiconductor components or packaged in the form of integrated

 doi:10.20944/preprints202504.2363.v1

circuits. Also, this method is small in size and low in cost, but is not suitable for high-power applications. Another active current equalization method is to add an additional switching converter to achieve current equalization by switching. The literatures [5,6] present that each string of LEDs is connected to the corresponding converter, and the output current of the converter is used to achieve current equalization of each string of LEDs, but its drawback is that the cost of the circuit is relatively high, and the control circuit is relatively complex. In the LED driver proposed in [7–9], a dimming switch is added to each LED string, and the duty cycle of the pulse width modulated (PWM) signal is adjusted to change the average value of current flowing through the LED string to achieve current equalization, whose disadvantage is that each LED string is connected in series with a switch, resulting in a larger number of switches and increasing the difficulty and complexity of design. Since the active current equalization method uses additional circuits, making the overall size larger, loss higher, control loop complex, etc., reducing the number of current detection circuits and regulation circuits is the goal of improving active current equalization.

Passive methods utilize the characteristics of passive components to achieve current equalization, and are divided into capacitor current equalization and transformer current equalization. The capacitor equalization method mentioned in [10] is when two different LED series have a voltage difference, the current equalization capacitor for charging and discharging is added, because the capacitor in the steady state has the characteristics of the ampere-second balance, that is to say, the average value of the capacitor current in a cycle is zero. The literature [11] shows a two-channel interleaved step-down LED driver using current equalization capacitors. In this circuit, the energy of the previous stage is transferred to the next LED driver through the current equalization capacitor, and thus part of the energy is consumed in the process of the transfer, which leads to relatively large current errors between the LEDs in the later stages. Moreover, every time a channel is expanded, an additional number of components close to the number of components needed for a buck circuit are used. The transformer current equalization method can be also a method used for current equalization of LED strings through the same turns of the transformer windings, and the primary and secondary sides of the transformer will be connected with two different LED strings. When the voltage of the LED string is unbalanced, a differential mode signal will be generated on the transformer, and the current equalization transformer will be activated to force the currents through the LED strings to be identical by utilizing the characteristics of the same number of turns on the primary and secondary sides. The current equalization circuit using differential-mode transformer proposed in the literatures [12,13] must add a freewheeling diodes or a zener diode to each LED string to ensure that the magnetic element has sufficient demagnetization voltage to make the switch completely demagnetized during the switch cutoff period, so the duty cycle of the switch will be limited.

Today's high power density LED driver circuits require switching power supplies to cope with the increased demand for LED loads. Although increasing the switching frequency of the switches can reduce the size of the passive components, the problems of switching loss and electromagnetic interference (EMI) become more serious with hard switching. In order to solve the above problems, the soft switching technology has been developed, which can be divided into zero voltage switching (ZVS) and zero current switching (ZCS), which can reduce the cross area between current and voltage during the switching period to minimize the switching loss. The literature [14] proposes a two-stage multi-channel LED driver, the front stage is a buck converter to regulate the rear CLL resonant converter, so that the latter can be operated at the resonant frequency through the primary-side coils of the transformers in series connection to achieve current equalization between the LED string modules, and in each LED string current equalization capacitor is added to balance the LED string module current flow in the opposite direction of the two LED strings. In order to expand the LED strings, more transformers are needed to be connected in series. The literature [15] proposes a step-down converter without any transformer, which operates in DCM mode with ZCS. At the same time, the amperage-second balance of the resonant capacitor is utilized to achieve the current equalization between the LED strings. In comparison, the difference between the literatures [16] and [15] is that

 doi:10.20944/preprints202504.2363.v1

the resonant current is operated in CCM and DCM, and the switch achieves ZVS turn-on when operated in CCM and ZCS turn-off when operated in DCM. The literature [17] proposes a LED driver that combines an LLC resonant converter and a current balancing circuit. A half-bridge LLC converter is used to provide the primary-side switches ZVS turn-on and the secondary-side rectifier diodes ZCS turn-off, and a current equalization capacitor is added to the secondary side to balance the current flowing through the LED strings. The literature [18] proposes an LCLC resonant LED driver, where the resonant tank of the LCLC can provide a relatively large ZVS range of the switch, and at the same time, reduce the current stress of the switch, and finally achieve the LED current regulation through the auxiliary switch. However, because the number of resonant components in this circuit is relatively large, there are several resonance points, causing the control of the range of operating frequency to be designed carefully. In addition to the original resonant topology, the ZCS turn-off applied to an additional auxiliary resonant circuit or snubber. The literature [19] adopts an interleaved buck-boost structure, consisting of two phases and adds one coupling inductor to replace the original two inductors, which are resonated with the parasitic capacitance of the main switch to realize the ZVS turn-on of the switch. In [20], a passive damping circuit is added to reduce the overlapping area of switching voltage and current during the switching period, so many passive components and diodes are added, resulting in additional losses. In addition, the auxiliary inductors in the damping circuit oscillate with the parasitic components of the switch during the switch cutoff period, resulting in additional switching losses. In [21], a dimmable LED driver based on H-bridge and differential-mode transformer are presented.

In this paper, a series resonant LED driver circuit based on differential-mode transformer current equalization is proposed. The proposed LED driver utilizes the characteristics of a differential-mode transformer to equalize the current flowing through each LED string. In the proposed circuit, the resonant circuit enables the half-bridge switch to realize ZVS turn-on. At the same time, when one even number of LED strings is increased, only one differential-mode transformer and one additional set of diodes need to be added, so that the number of parts used can be reduced. The purpose of this paper is to improve the magnetic resetting of the differential-mode transformer. Compared with [12], the circuit proposed in this paper is not limited by the duty cycle of the gate driving signals for the main switches, so that a higher load regulation range can be achieved.

2. System Configuration

Figure 1 shows the series resonant LED driver circuit based on the differential-mode transformer current equalization, the main structure uses a half-bridge series resonant converter. The feedback circuit uses a current sensor to obtain the current feedback signal from one of the LED strings, which is sent to the analog-to-digital converter (ADC) inside the DSP. Afterwards, this sensed feedback signal is subtracted from the current reference to obtain the corresponding error signal through the DSP algorithm calculation. After this, the corresponding control force can be obtained, and finally the control force is transferred to variable frequency and sent to the half-bridge switches S_1 and S_2 through an isolated half-bridge gate driver to control these two switches.

 doi:10.20944/preprints202504.2363.v1

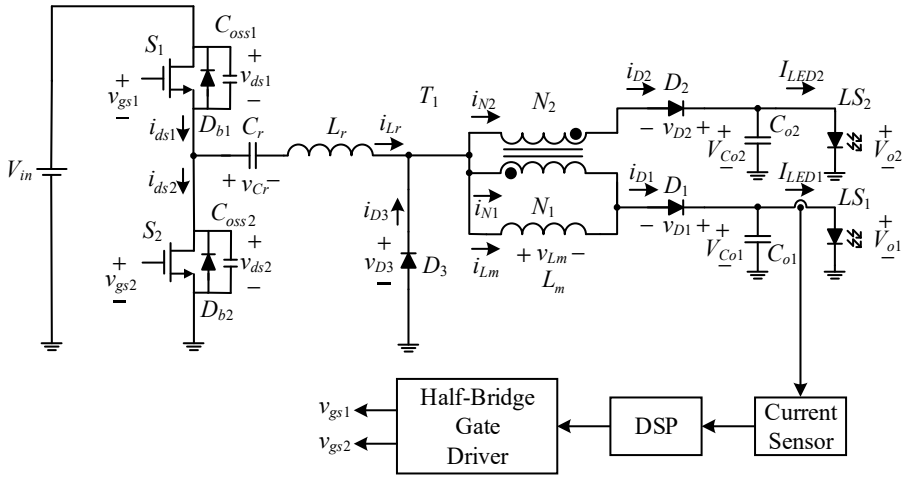

Figure 1. System configuration of the proposed circuit.

As shown in Figure 1, the circuit consists of two switches S_1 and S_2, a resonant inductor L_r and a resonant capacitor C_r formed by the series resonant tank, with the function of current equalization based on differential-mode transformer T_1, which is composed of a magnetizing inductor L_m, a primary-side coil N_1, a secondary-side coil N_2, the primary-side and secondary-side leakage inductances L_{lk1} and L_{lk2}, respectively, the two rectifier diodes D_1 and D_2, and the freewheeling diode D_3. In addition, the load side is composed of two LED strings LS_1 and LS_2, and two output capacitors C_{o1} and C_{o2}.

3. Operating Principle

Before introducing the analysis of the circuit behavior, there are some assumptions and symbol definitions:

(1) V_{in} is the input voltage; LS_1 and LS_2 are the output LED strings and the voltages on them are equal to the output voltages V_{o1} and V_{o2}, respectively.

(2) S_1 and S_2 are the switches of the upper and lower switches of the half-bridge, D_{b1} and D_{b2} are the body diodes of the switches S_1 and S_2, respectively, C_{oss1} and C_{oss2} are the output capacitances of the switches S_1 and S_2, respectively, and the corresponding forward conduction voltages are assumed to be zero.

(3) The characteristics of rectifier diodes D_1 and D_2 and magnetic resetting diode D_3 are ideal.

(4) The coupling coefficient of the differential-mode transformer is one, i.e., only the magnetizing inductance L_m is taken into account, and the leakage inductances L_{lk1} and L_{lk2} are ignored.

(5) The output capacitors C_{o1} and C_{o2} are large enough to be considered as constant.

(6) The current through the resonant inductor L_r is i_{Lr}, and the voltage on the resonant capacitor C_r is v_{Cr}.

(7) v_{ds1} is the voltage on the switch S_1, v_{ds2} is the voltage on the switch S_2, v_{D1} is the voltage on the diode D_1, v_{D2} is the voltage on the diode D_2, v_{D3} is the voltage on the diode D_3, and v_{Lm} is the voltage on the magnetizing inductance L_m.

(8) i_{ds1} is the current flowing through the switch S_1, i_{ds2} is the current flowing through the switch S_2, i_{D1} is the current flowing through the diode D_1, i_{D2} is the current flowing through the diode D_2, i_{D3} is the current flowing through the diode D_3, i_{N1} is the primary-side current of the differential-mode transformer T_1, i_{N2} is the secondary-side current of the differential-mode transformer, i_{Lm} is the current flowing through the magnetizing inductance L_m, I_{LED1} is the current flowing through the first LED string LS_1, and I_{LED2} is the current through the second LED string LS_2.

(9) v_{gs1} and v_{gs2} are the driving signals for upper arm the switches S_1 and S_2 respectively.

(10) T_s is the switching period, and f_s is the switching frequency.

Figure 2 shows key waveforms relevant to the proposed circuit.

 doi:10.20944/preprints202504.2363.v1

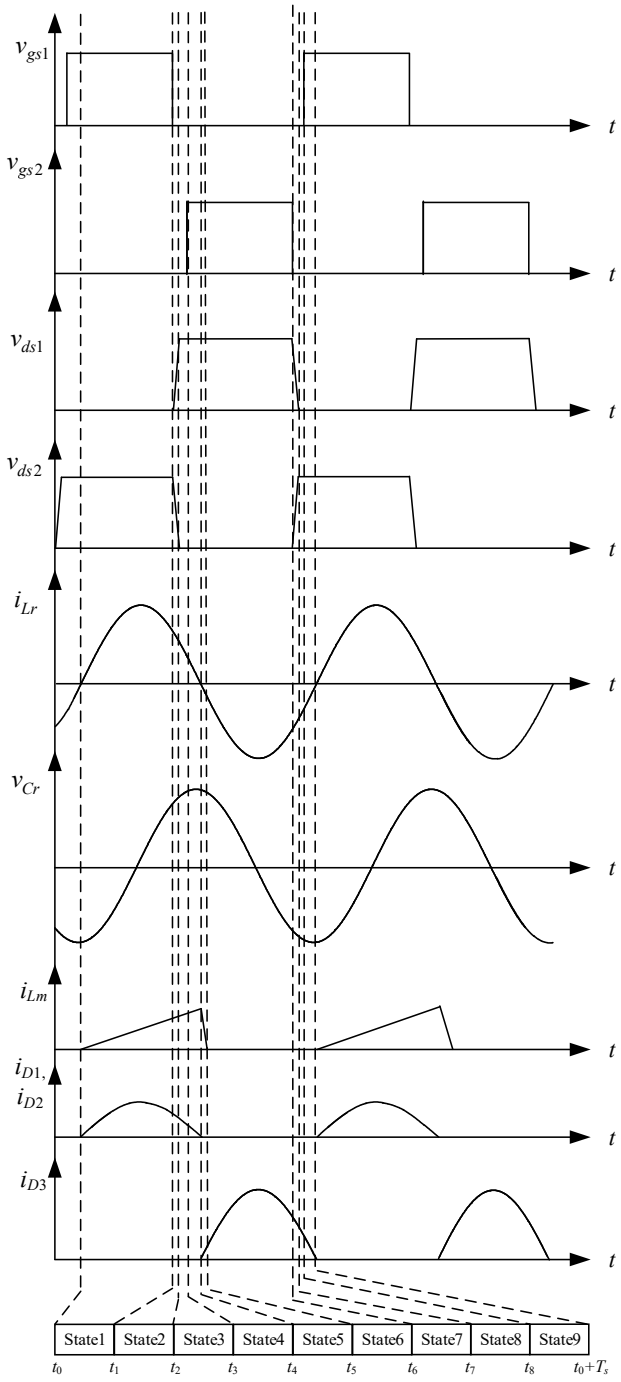

Figure 2. Key waveforms relevant to the proposed circuit.

State 1. $[t_0 \le t < t_1]$: As shown in Figure 3a, the switch S_1 is on, the switch S_2 is off, and the resonant inductor current i_{Lr} resonates from negative to zero. Sequentially, the resonant inductor L_r and the resonant capacitor C_r resonate with each other, and the resonant inductor current i_{Lr} starts to flow positively from zero. The current flows from the input V_{in}, through the switch S_1, the resonant capacitor C_r, the resonant inductor L_r, the diodes D_1 and D_2, and the differential-mode transformer T_1 to the LED strings LS_1 and LS_2. If there is a voltage difference between the two LED strings, the differential-mode transformer is activated, and the voltage on L_m, called v_{Lm}, is clamped at half of the difference in voltage between the two LED strings, and the magnetizing inductance L_m starts to be linearly excited. Once the switch S_1 cuts off, the circuit enters state 2.

 doi:10.20944/preprints202504.2363.v1

State 2. $[t_1 \le t < t_2]$: As shown in Figure 3b, the switches S_1 and S_2 are off. During this state, the resonant inductor current i_{Lr} still flows positively, and the current flows to the LED strings LS_1 and LS_2 through the differential-mode transformer T_1 and the freewheeling diodes D_1 and D_2. In this state, the operation of the differential-mode transformer T_1 and the two LED strings LS_1 and LS_2 is the same as that in the previous state. Since both of the switches are in the off-and the resonant current i_{Lr} must continue, the resonant inductor current i_{Lr} is the same as that in the previous state. The resonant inductor current i_{Lr} charges the output capacitor C_{oss1} of the switch S_1 and discharges the output capacitor C_{oss2} of the switch S_2, respectively. The moment the output C_{oss1} is charged to the input voltage V_{in} and the output C_{oss2} is discharged to zero, the circuit enters state 3.

State 3. $[t_2 \le t < t_3]$: As shown in Figure 3c, the switches S_1 and S_2 are still cutoff. During this state, the output capacitor C_{oss2} of the switch S_2 has been discharged to zero, causing the body diode D_{b2} of the switch $0S_2$ to conduct, and the resonant inductor current i_{Lr} is still positively flowing and gradually decreasing. In this state, the differential-mode transformer T_1 and the two LED series LS_1 and LS_2 operate as in the previous state. Once the switch S_2 is turned on, the circuit enters state 4.

State 4. $[t_3 \le t < t_4]$: As shown in Figure 3d, the switch S_1 is still off and the switch S_2 is on. During this state, since the body diode of S_2 has been first conducted in the previous state, the voltages across the switches S_1 and S_2 are close to zero, so the switch S_2 is turned with ZVS. In addition, the resonant inductor current i_{Lr} flows in the positive direction and decreases gradually. In this state, the differential-mode transformer T_1 and the LED strings LS_1 and LS_2 operate as in the previous state. As soon as the resonant inductor current i_{Lr} decreases to zero and the circuit enters state 5.

State 5. $[t_4 \le t < t_5]$: As shown in Figure 3e, the switch S_1 remains off and the switch S_2 remains on. During this state, the resonant inductor current i_{Lr} starts to flow from zero in the opposite direction. In addition, the magnetizing inductor L_m of the differential-mode transformer T_1 is demagnetized through the freewheeling diode D_1 and the magnetic resetting diode D_3, so the magnetizing inductance current i_{Lm} decreases linearly. Note that this experienced time in this state is much smaller than half of the switching period. Once the magnetizing inductance current i_{Lm} drops to zero, the circuit proceeds to state 6.

State 6. $[t_5 \le t < t_6]$: As shown in Figure 3f, the switch S_1 is still off and the switch S_2 is continuously on. During this state, the resonant inductor current i_{Lr} flows negatively through the diode D_3. In addition, since the magnetizing inductor current i_{Lm} has been demagnetized to zero, so the freewheeling diodes D_1 and D_2 are both cut off and there is no energy sent to the output side. Therefore, the energy required for the LED strings LS_1 and LS_2 is supplied by the output capacitors C_{o1} and C_{o2}, respectively. The moment the switch S_2 is cut off, the circuit enters state 7.

State 7. $[t_6 \le t < t_7]$: As shown in Figure 3g, the switches S_1 and S_2 are cut off. During this state, the resonant inductor current i_{Lr} still flows negatively through D_3, and the freewheeling diodes D_1 and D_2 are still cut off. In addition, the operation of the differential-mode transformer T_1 and the output is the same as the previous state. Since the switches S_1 and S_2 are off, the resonant inductor current i_{Lr} discharges C_{oss1} and charges C_{oss2}. As soon as the output capacitance C_{oss1} discharges to zero and the output capacitance C_{oss2} charges to V_{in}, the circuit enters state 8.

State 8. $[t_7 \le t < t_8]$: As shown in Figure 3h, the switches S_1 and S_2 are in the off-state. During this state, since the output capacitor C_{oss1} of the switch S_1 has been discharged to zero, the body diode D_{b1} of the switch is on, and the resonant inductor current i_{Lr} flows through the diode D_3, the resonant inductor L_r, the resonant capacitor C_r, the body diode D_{b1} of the switch S_1, and the input. In addition, the differential-mode transformer and the two LED strings LS_1 and LS_2 operate in the same way as in the previous state. Once the upper arm switch S_1 turns on and enters state 9.

State 9. $[t_8 \le t < t_0 + T_s]$: As shown in Figure 3i, the switches S_1 is on and the switch S_2 is off. During this state, since the body diode D_{b1} of the switch has been on in the previous state, the switch S_1 can realize ZVS turn-on, and the resonant inductor current i_{Lr} flows negatively and rises continuously. In addition, the differential-mode transformer and the two LED series LS_1 and LS_2

 doi:10.20944/preprints202504.2363.v1

operate as in the previous state. The moment the resonant inductor current i_{Lr} rises to zero, the circuit proceeds to the next cycle.

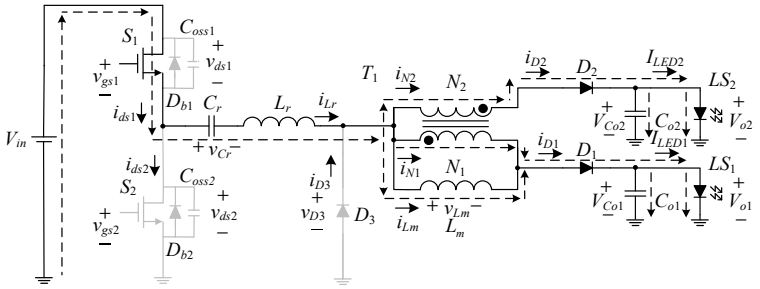

(a)

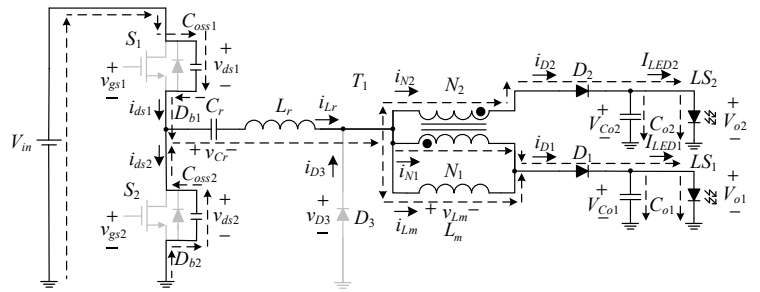

(b)

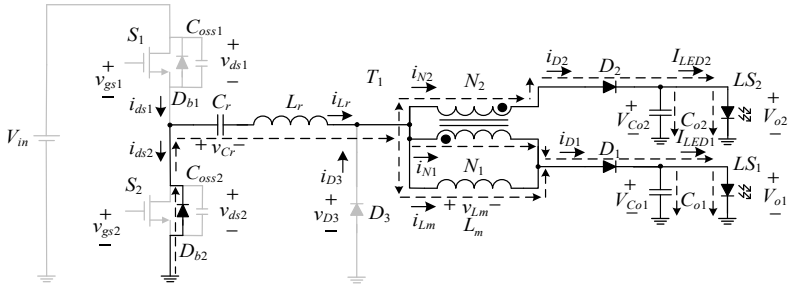

(c)

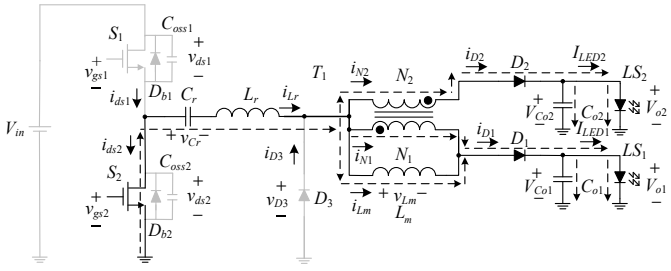

(d)

 doi:10.20944/preprints202504.2363.v1

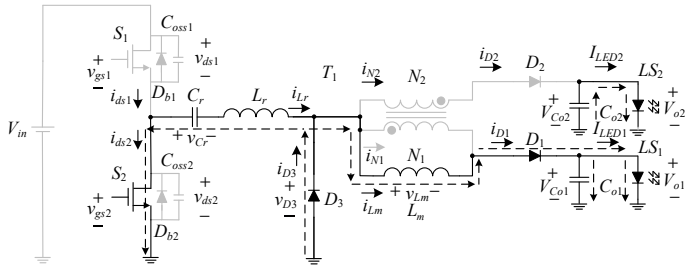

(e)

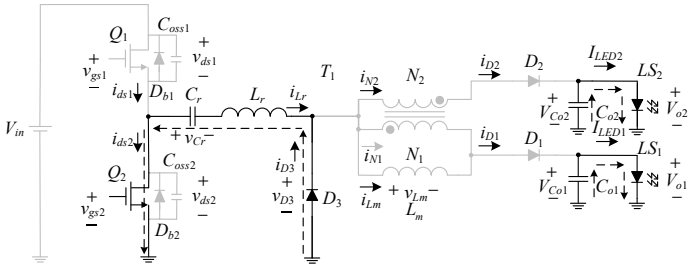

(f)

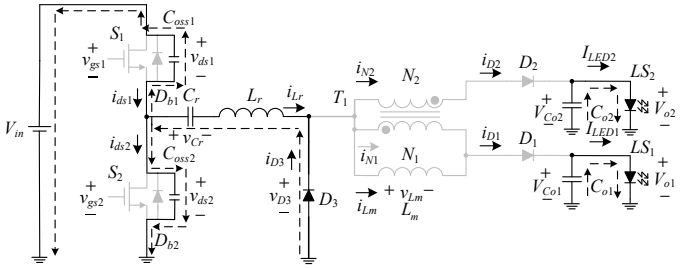

(g)

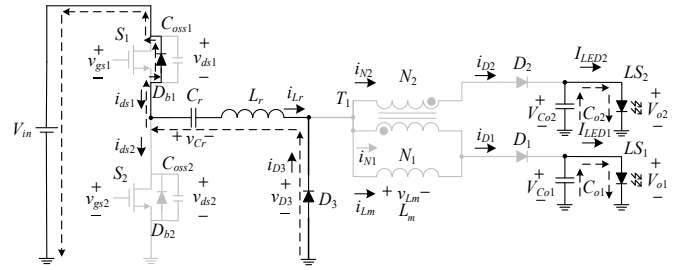

(h)

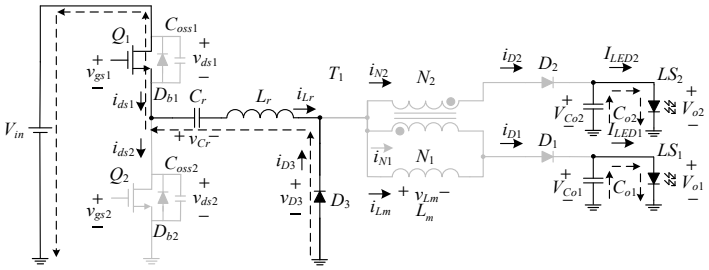

(i)

 doi:10.20944/preprints202504.2363.v1

Figure 3. Current flow: (a) state 1; (b) state 2; (c) state 3; (d) state 4; (e) state 5; (f) state 6; (g) state 7; (h) state 8; (i) state 9.

3.1. Voltage Gain

The first harmonic approximation (FHA) is utilized herein to find the equivalent output AC load resistance $R_{o,ac}$, reflected from the secondary side to the primary side, to be derived as follows.

First, the average value $I_{Lr,avg}$ of the half-cycle resonant current i_{Lr} is the sum of the currents in the two LED strings, equal to the total output current I_o:

$$I_{Lr,avg} = I_{LED1} + I_{LED2} = I_o \tag{1}$$

Also, the peak value $I_{Lr,peak}$ and RMS value $I_{L,rms}$ of the resonant current i_{Lr} can be expressed as follows:

$$I_{Lr,peak} = I_o \times \pi \tag{2}$$

$$I_{Lr,rms} = I_{Lr,peak} \times \frac{1}{\sqrt{2}} = \frac{\pi \times I_o}{\sqrt{2}} \tag{3}$$

The output voltage v_o of the resonant tank is the voltage on the diode D_3, which is a unipolar square wave, that is,

$$\begin{aligned} v_o(t) &= v_{D3}(t) = V_o, \quad i_{Lr}(t) > 0 \\ v_o(t) &= v_{D3}(t) = 0\ , \quad i_{Lr}(t) < 0 \end{aligned} \tag{4}$$

Thus, the fundamental RMS value $V_{o,FHA,rms}$ of the output voltage v_o of the resonant tank is

$$V_{o,FHA,rms} = \frac{\sqrt{2} \times V_o}{\pi} \tag{5}$$

Eventually, dividing (5) by (3) yields

$$R_{o,ac} = \frac{V_{o,FHA,rms}}{I_{Lr,rms}} = \frac{\frac{\sqrt{2} \times V_o}{\pi}}{\frac{\pi \times I_o}{\sqrt{2}}} = \frac{2}{\pi^2}\frac{V_o}{I_o} = \frac{2R_o}{\pi^2} \tag{6}$$

On the other hand, the input voltage v_{in} of the resonant can be expressed as

$$\begin{aligned} v_{in}(t) &= v_{ds2}(t) = V_{in}, \quad 0 \le t \le \frac{T_s}{2} \\ v_{in}(t) &= v_{ds2}(t) = 0\ , \quad \frac{T_s}{2} \le t \le T_s \end{aligned} \tag{7}$$

Therefore, the RMS value of the fundamental wave of v_{in} is

$$V_{in,FHA,rms} = \frac{2V_{in}}{\pi} \times \frac{1}{\sqrt{2}} = \frac{\sqrt{2}}{\pi} V_{in} \tag{8}$$

From the above derivation, the relationship between the input fundamental waveform and the output fundamental waveform of the resonant tank can be found. By using (5) and (8), the DC gain M_{dc} of the circuit can be expressed by

$$M_{dc} = \frac{V_{o,FHA,rms}}{V_{in,FHA,rms}} = \frac{\frac{\sqrt{2} \times V_o}{\pi}}{\frac{\sqrt{2} \times V_{in}}{\pi}} = \frac{V_o}{V_{in}} \tag{9}$$

 doi:10.20944/preprints202504.2363.v1

According to (3), (5) and (8), the s-domain equivalent circuit of the proposed circuit is shown in Figure 4.

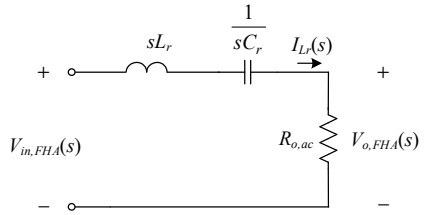

Figure 4. s-domain equivalent of the proposed circuit.

According to Figure 4, the voltage gain $M(s)$ of the circuit is given by

$$M(s)=\frac{V_{o,FHA}(s)}{V_{in,FHA}(s)}=\frac{R_{o,ac}}{sL_r+\frac{1}{sC_r}+R_{o,ac}} \tag{10}$$

The defined resonant radian frequency ω_r, the characteristic impedance Z_r, and the quality factor Q are

$$\omega_r=\frac{1}{\sqrt{L_rC_r}},\quad Z_r=\sqrt{\frac{L_r}{C_r}},\quad Q=\frac{Z_r}{R_{o,ac}} \tag{11}$$

Substituting (11) into (10) yields

$$M(s)=\frac{\frac{s}{\omega_r}\times\frac{1}{Q}}{(\frac{s}{\omega_r})^2+\frac{s}{\omega_r}\frac{1}{Q}+1} \tag{12}$$

Substituting $s=j\omega_s=j2\pi f_s$ and $\omega_r=j2\pi f_r$ into (10) and letting $M=\left|M(j2\pi f_s)\right|$, the voltage gain M of the proposed circuit is given by

$$M=\frac{V_o}{V_{in}}=\frac{1}{\sqrt{Q^2\left[\left(\frac{f_r}{f_s}\right)^2+\left(\frac{f_s}{f_r}\right)^2-2\right]+1}} \tag{13}$$

Figure 5 shows the curve of voltage gain M versus the ratio of switching frequency f_s to resonant frequency f_r for different values of quality factor Q. In the case of a fixed resonant elements, the smaller the load resistance is, the larger the value of Q is, the curve of the voltage gain M is steeper, and the voltage gain is more likely to be caused by the change of frequency, so the stability of the system is poorer but the response speed of voltage regulation is faster. On the contrary, the smaller the value of Q is, the larger the frequency change range is needed to stabilize the output voltage.

 doi:10.20944/preprints202504.2363.v1

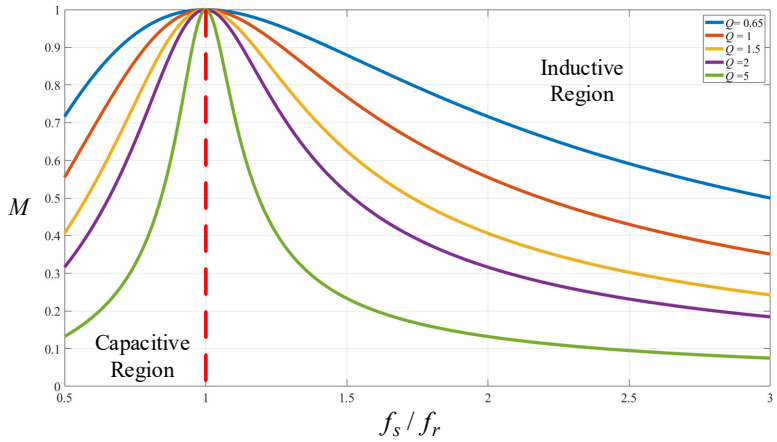

Figure 5. Voltage gain curve of the proposed circuit.

Figure 6 shows the current equalization circuit of the differential-mode transformer T_1, where N_1 and N_2 are the primary and secondary windings of the differential-mode transformer T_1 with N_1 equal to N_2, L_m is the primary-side magnetizing inductance, and LED_1 and LED_2 are the loads connected in series to N_1 and N_2, respectively. In addition, i_{N1} and i_{N2} are the primary-side and secondary-side currents of T_1, respectively. i_{Lm} is the current flowing through the magnetizing inductance L_m, v_1 and v_2 are the primary-side and secondary-side voltages of T_1, respectively, and v_{Lm} is the voltage on the magnetizing inductance L_m of T_1.

Since the turns ratio is one and the polarity dots are in the opposite direction, the following are the results

$$v_{Lm} = v_1 = v_2 \tag{14}$$

$$i_{N1} = i_{N2} \tag{15}$$

In Figure 6, according to Kirchhoff's voltage law, it can be known that

$$v_1 + V_{LED1} = -v_2 + V_{LED2} \tag{16}$$

When two LED strings have the same voltages on them, i.e., V_{LED1}=V_{LED2}, according to (14) and (16), there is no voltage on the differential-mode transformer T_1, i.e., T_1 is not activated. When a voltage imbalance occurs, a balancing voltage on the magnetizing inductance is generated, as shown in (17). Accordingly, T_1 is activated, forcing the primary and secondary sides of T_1 to have the same currents, i.e., equalizing the currents in LED_1 and LED_2 due to the turns ratio of one.

$$v_{Lm} = \frac{V_{LED2} - V_{LED1}}{2} \tag{17}$$

However, in practice, there must be a magnetizing inductance L_m. Therefore, in the case of voltage imbalance, the balanced voltage will energize the magnetizing inductance and generate the magnetizing current i_{Lm}, and the average value of this current will be the current error between the two LED strings. In Figure 6, according to Kirchhoff's current law, it can be seen that

$$i_{LED1} = i_{N1} + \mathrm{i}_{Lm} \tag{18}$$

$$i_{LED2} = i_{N2} \tag{19}$$

Accordingly, in the process of current equalization, the current in the magnetizing inductance L_m of T_1, called i_{Lm}, will cause the current equalization error.

 doi:10.20944/preprints202504.2363.v1

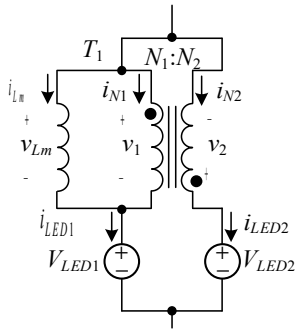

Figure 6. Current equalization circuit based on the differential-mode transformer.

From Section 3, it can be seen that the magnetizing inductance L_m is linearly excited in states 1 to 4 ($t_0 \le t < t_4$) and the voltage v_{Lm} is $0.5\times(V_{o1}-V_{o2})$. In state 5, the magnetizing inductance L_m is linearly demagnetized, and the voltage v_{Lm} is $-V_{o1}$. Figure 7 shows the operating behavior of the magnetizing inductance.

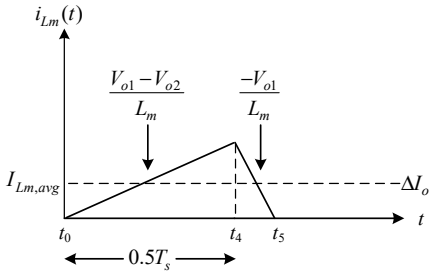

Figure 7. Operating behavior of magnetizing inductance.

$$\Delta I_o = \frac{\Delta V}{16\times L_m \times f_s}$$
$$\Rightarrow L_m = \frac{\Delta V}{16\times f_s \times \left[\frac{2\times I_{LED1}}{1-\varepsilon} - 2\times I_{LED1}\right]} \tag{20}$$

From Figure 7, the elapsed time of the magnetizing inductance L_m is $0.5T_s$, and the magnetization voltage is much smaller than the demagnetization voltage. So, the demagnetization time can be ignored, and the average value of the magnetizing inductance current, called $I_{Lm,avg}$, can be expressed as

$$I_{Lm,avg} = \Delta I_o = \frac{1}{T_s}\left(\frac{1}{2}\times\frac{\Delta V}{2L_m}\times 0.5T_s \times 0.5T_s\right)$$
$$= \frac{\Delta V}{16\times L_m \times f_s} \tag{21}$$

where ΔV is the difference in voltage between the two LED strings, namely, $V_{o1}-V_{o2}$.

After that, the average I_{avg} of the currents of the two LED strings can be expressed by

$$I_{avg} = \frac{I_{LED1}+I_{LED2}}{2} \tag{22}$$

Substituting (18) and (19) into (22) yields

 doi:10.20944/preprints202504.2363.v1

$$I_{avg} = \frac{I_{LED1} + I_{LED2}}{2} = \frac{I_{N1} + \Delta I_o + I_{N2}}{2} = \frac{2I_{LED1} - \Delta I_o}{2} \tag{23}$$

Sequentially, the current sharing error percentage ε is defined to be

$$\varepsilon = \frac{\left|I_{avg} - I_{LED1}\right|}{I_{avg}} \times 100\% = \frac{\left|I_{avg} - I_{LED2}\right|}{I_{avg}} \times 100\% \tag{24}$$

By substituting (23) into (24), the current error ΔI_o can be expressed as

$$\Delta I_o = \frac{2 \times I_{LED1}}{1-\varepsilon} - 2 \times I_{LED1} \tag{25}$$

By substituting (25) into (20), the relationship between the current error percentage and the magnetizing inductance L_m can be obtained to be

$$\Delta I_o = \frac{\Delta V}{16 \times L_m \times f_s} \Rightarrow L_m = \frac{\Delta V}{16 \times f_s \times \left[\frac{2 \times I_{LED1}}{1-\varepsilon} - 2 \times I_{LED1}\right]} \tag{26}$$

4. Design Considerations

The system specifications of the proposed circuit are shown in Table 1.

Table 1. System specifications.

Rated Input Voltage (V_{in})	48V
Rated Output Voltage ($V_{o,rated}$)	32V (10 units in a string)
Rated Output Current ($I_{o,rated}$)	0.7A
Rated Output Power ($P_{o,rated}$)	22.4W (10LEDs,10LEDs)
Unbalanced Output Power ($P_{o,unbalanced}$)	20.16W (10 LEDs, 8LEDs)
Resonant Frequency (f_r)	100kHz
Quality Factor (Q)	2
Absolute current error percentage ($\left\|\varepsilon\right\|$)	<1%

Since the rated-load voltage of a single LED is about 3.2V, the output rated voltage $V_{o,rated}$ on a LED string is 32V, which is constructed by the voltage of 10 LEDs in series. In the case of unbalanced output, the two LED strings are composed of 10 LEDs in series and 8 LEDs in series, respectively. The current error percentage between the two LED strings must be less than 1% from 25% to 100% of the load.

In this section, the parameters of the resonant tank, differential-mode transformer, and output capacitor will be designed.

4.1. Equivalent Output AC Load Resistance $R_{o,ac}$

According to Table 4, the value of R_o is

$$R_o = \frac{V_{o,rated}}{I_{o,rated}} = \frac{32}{0.7} \cong 45.7\Omega \tag{27}$$

 doi:10.20944/preprints202504.2363.v1

Therefore, the value of $R_{o,ac}$ can be found according to (6), that is,

$$R_{o,ac} = \frac{2R_o}{\pi^2} = \frac{2\times 54.7}{\pi^2} \cong 9.27\Omega \tag{28}$$

4.2. Resonant Components L_r and C_r

By considering the range of operating frequency and the stability of system control, the value of Q is set at 2. By substituting the resonant frequency of 100kHz in Table 1 into (11), the value of resonant capacitor C_r can be obtained first:

$$\begin{aligned} Q &= \frac{1}{2\times\pi\times f_r\times R_{o,ac}\times C_r} \\ \Rightarrow C_r &= \frac{1}{2\times\pi\times f_r\times R_{o,ac}\times Q} \\ &= \frac{1}{2\times\pi\times 100\times 10^3\times 9.27\times 2} = 85.8\text{nF} \end{aligned} \tag{29}$$

Therefore, a plastic capacitor of 82nF is selected and close to the calculated value. Afterwards, the value of the resonant capacitor C_r and the value of the resonant frequency f_r are used to find the value of the resonant inductor L_r:

$$\begin{aligned} f_r &= \frac{1}{2\times\pi\times\sqrt{L_r\times C_r}} \\ \Rightarrow L_r &= \frac{1}{(2\times\pi\times f_r)^2\times C_r} \\ &= \frac{1}{(2\times\pi\times 100\times 10^3)\times 82\times 10^{-9}} = 30.92\mu\text{H} \end{aligned} \tag{30}$$

Accordingly, the actual value of Q is 2.09 based on the selected elements of the resonant tank.

4.3. Magnetizing Inductance L_m

By using the simulation software PSIM 9.11, the voltages V_{o1} and V_{o2} of the two LEDs at 25% load are 28.98V and 22.42V, respectively. Meanwhile, the voltage gain $M_{(25\%)}$ M1and quality factor $Q_{(25\%)}$ at 25% load are as follows:

$$M_{(25\%)} = \frac{V_o}{V_{in}} = \frac{\frac{28.98+22.42}{2}}{48} = 0.54 \tag{31}$$

$$1\,Q_{(25\%)} = \frac{Z_r}{R_{o.ac(25\%)}} = \frac{\sqrt{\frac{30.89\times 10^{-6}}{82\times 10^{-9}}}}{\frac{2\times 25.74}{\pi^2\times 0.7\times 0.25}} = 0.65 \tag{32}$$

where V_o is the average voltage of voltages on the two LED strings.

By substituting (31) and (32) into (13), the relationship between the resonant frequency f_r divided by the switching frequency f_s at 25% load can be approximately obtained to be

 doi:10.20944/preprints202504.2363.v1

$$M_{(25\%)} = \frac{1}{\sqrt{Q^2\left[\left(\frac{f_r}{f_s}\right)^2 + \left(\frac{f_s}{f_r}\right)^2 - 2\right] + 1}}$$
$$\Rightarrow 0.53 = \frac{1}{\sqrt{0.65^2\left[\left(\frac{f_r}{f_s}\right)^2 + \left(\frac{f_s}{f_r}\right)^2 - 2\right] + 1}} \quad (33)$$
$$\Rightarrow \frac{f_r}{f_s} = \pm 2.76 \text{ 、 } \pm 0.36$$

Therefore, the ratio of resonance frequency f_r to switching frequency f_s is 0.36, which corresponds to a switching frequency of 276 kHz.

By substituting the result of (32) and the relevant specifications in Table 1 into (25), the required magnetizing inductance L_m at 25% load with current error percentage less than 1% can be obtained to be

$$L_m \geq \frac{\Delta V}{16 \times f_s \times \left[\frac{2 \times I_{LED1}}{1-\varepsilon} - 2 \times I_{LED1}\right]}$$
$$\geq \frac{28.98 - 22.42}{16 \times 277 \times 10^3 \times \left[\frac{2 \times 0.35 \times 0.25}{1 - 0.01} - (2 \times 0.35 \times 0.25)\right]} \quad (34)$$
$$\geq 840\mu\text{H}$$

Finally, the value of the magnetizing inductance L_m is set at 1.05mH.

4.4. Channel Extension

Figure 8 shows the four-channel LED strings, which only needs to add two differential-mode transformers, two diodes and two output capacitors to achieve this goal. It is worth mentioning that the equivalent AC resistance needs to be recalculated when the number of LED strings are increased.

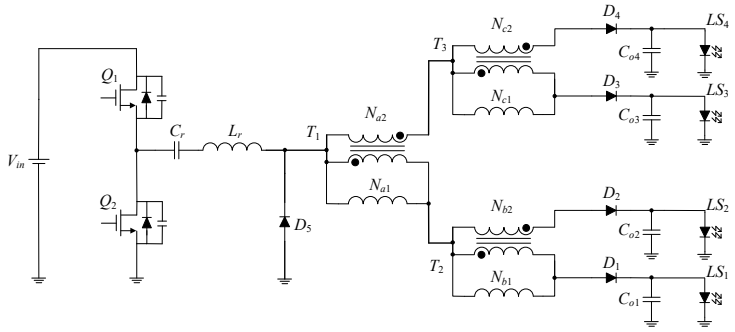

Figure 8. Four-channel LED circuit.

5. Experimental Results

In the following, the waveforms at 100% and 25% loads, the current error percentage, the overall efficiency, and the variable switching frequency are measured.

5.1. Waveforms at 100% Load

Figures 9–15 show the measured waveforms at 100% load.

 doi:10.20944/preprints202504.2363.v1

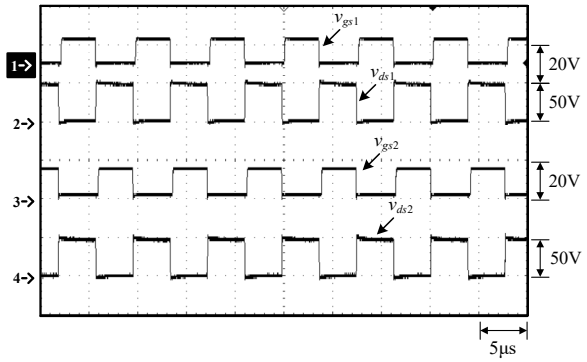

Figure 9. Waveforms at 100% load: (1) v_{gs1}; (2) v_{ds1}; (3) v_{gs2}; (4) v_{ds2}.

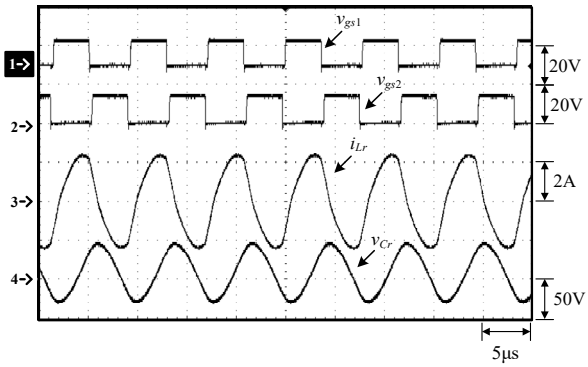

Figure 10. Waveforms at 100% load: (1) v_{gs1}; (2) v_{gs2}; (3) i_{Lr}; (4) v_{Cr}.

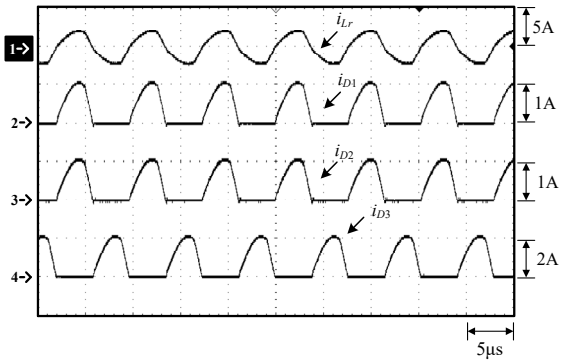

Figure 11. Waveforms at 100% load: (1) i_{Lr}; (2) i_{D1}; (3) i_{D2}; (4) i_{D3}.

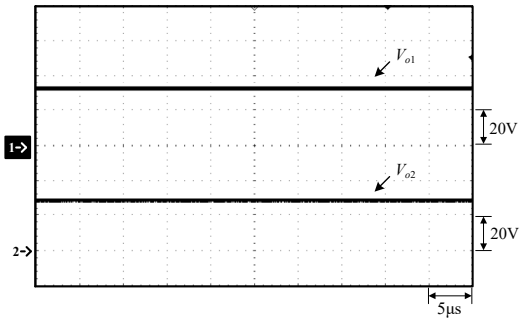

Figure 12. Waveforms at 100% load: (1) V_{o1}; (2) V_{o2}.

 doi:10.20944/preprints202504.2363.v1

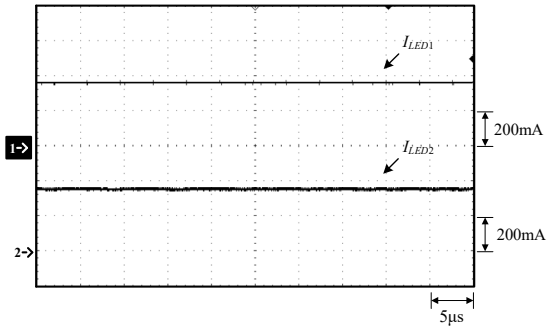

Figure 13. Waveforms at 100% load: (1) I_{LED1}; (2) I_{LED2}.

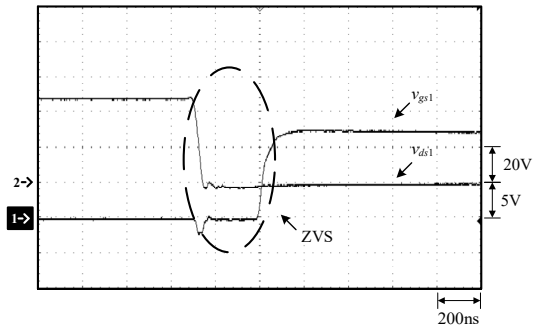

Figure 14. Waveforms at 100% load: (1) v_{gs1}; (2) v_{ds1}.

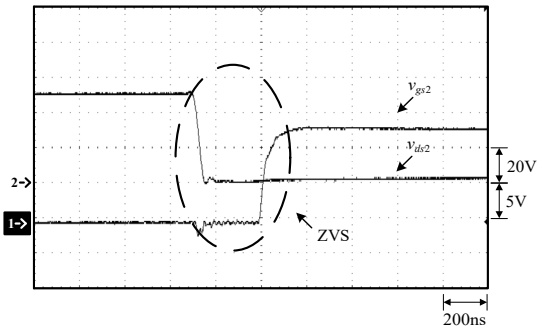

Figure 15. Waveforms at 100% load: (1) v_{gs2}; (2) v_{ds2}.

5.2. Waveforms at 25% Load

Figures 16–22 show the measured waveforms at 25% load.

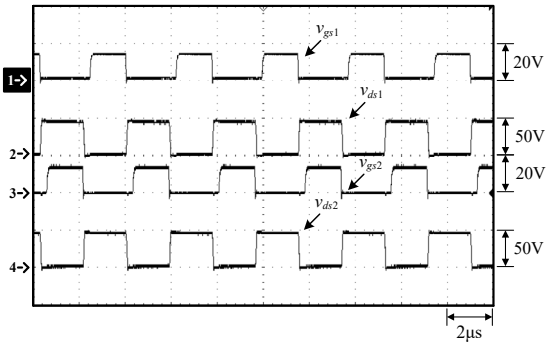

Figure 16. Waveforms at 25% load: (1) v_{gs1}; (2) v_{ds1}; (3) v_{gs2}; (4) v_{ds2}.

 doi:10.20944/preprints202504.2363.v1

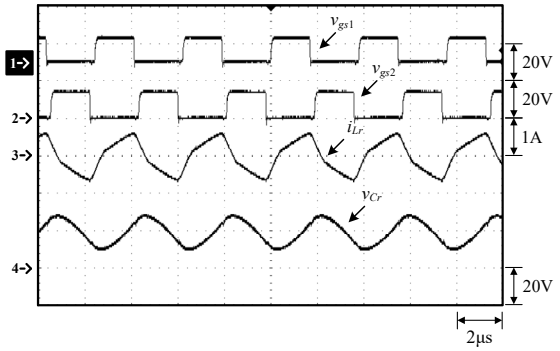

Figure 17. Waveforms at 25% load: (1) v_{gs1}; (2) v_{gs2}; (3) i_{Lr}; (4) v_{Cr}.

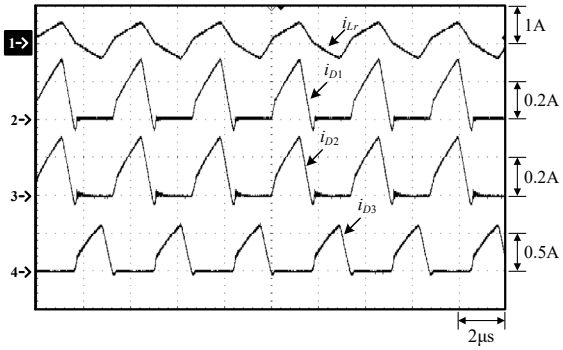

Figure 18. Waveforms at 25% load: i_{Lr}; (2) i_{D1}; (3) i_{D2}; (4) i_{D3}.

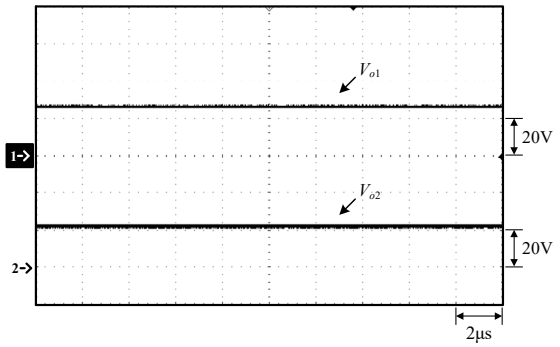

Figure 19. Waveforms at 25% load: (1) V_{o1}; (2) V_{o2}.

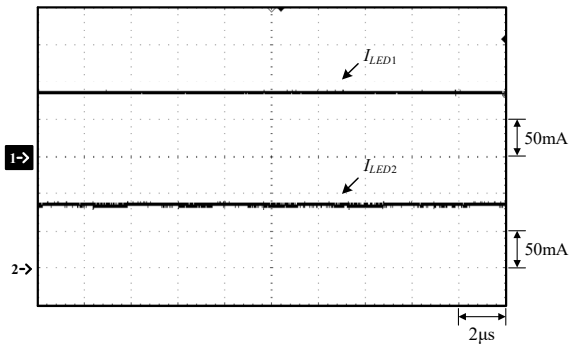

Figure 20. Waveforms at 25% load: (1) I_{LED1}; (2) I_{LED2}..

 doi:10.20944/preprints202504.2363.v1

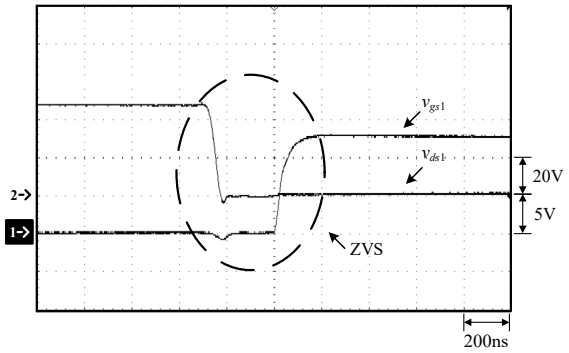

Figure 21. Waveforms at 25% load: (1) v_{gs1}; (2) v_{ds1}.

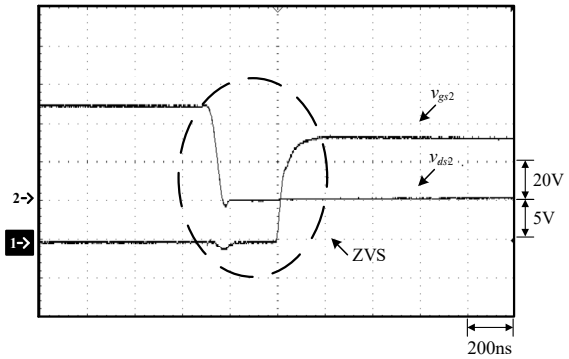

Figure 22. Waveforms at 25% load: (1) v_{gs2}; (2) v_{ds2}.

From Figures 10, 11, 17 and 18, it can be seen that when the resonant inductor current i_{Lr} is in the positive direction, the resonant inductor L_r resonates with the resonant capacitor C_r, and at the same time the resonant inductor current i_{Lr} is equally distributed to the diode currents i_{D1} and i_{D2} through the differential-mode transformer, while the diode D_3 is in the off-state so the diode current i_{D3} is zero. When the resonant inductor current i_{Lr} enters the negative flow direction, both the diodes D_1 and D_2 are cut off, so i_{D1} and i_{D2} are zero. Since the diode D_3 is on, the resonant inductor current i_{Lr} continues to flow through the diode D_3 and hence no energy is transferred to the output. In addition, as the switching frequency moves away from the resonant frequency, the resonant inductor current i_{Lr} gradually becomes more linear, different from the sine wave.

From Figures 12, 13, 19 1nd 20, it can be seen that for any current load, even if the voltages of the LED strings are different due to different numbers of LEDs, the effect of current equalization can be achieved and the constant current output can be maintained.

As can be seen in Figures 14 and 21, before the switch S_1 is turned on, the voltage v_{ds1} of the switch S_1 has dropped to zero and hence the switch S_1 is with ZVS turn-on. As can be seen in Figures 15 and 22, before the switch S_2 is turned on, the voltage v_{ds2} of the switch S_1 has dropped to zero and hence the switch S_2 is with ZVS turn-on.

5.3. Current Error Percentage of LED Strings

In this subsection, the measured data of the proposed circuit are used to calculate the current sharing error percentage (CSEP, ε) of the LED strings at different loads:

$$\varepsilon = \left| \frac{I_{\mathrm{LED}y} - \frac{1}{n}\sum_{x=1}^{n} I_{LEDx}}{\frac{1}{n}\sum_{x=1}^{n} I_{LEDx}} \right| \times 100\% \tag{35}$$

 doi:10.20944/preprints202504.2363.v1

where ε is the current error percentage of LED strings, n is the number of LED strings, and I_{LEDy} is the current of the yth LED string, and $\sum_{x=1}^{n} I_{LEDx}$ is the sum of currents in all LED strings.

Tables 2 and 3 show the measurement data of 100% and 25% load, respectively, where the LED string LS_1 has 10 LEDs in series and the LED string LS_2 has 8 LEDs in series.

Table 2. Measurement data at 100% load.

	LS_1	LS_2
I_{LED} (mA)	351.2	353.1
V_{LED} (V)	31.68	25.3

Table 3. Measurement data at 25% load.

	LS_1	LS_2
I_{LED} (mA)	85.50	87.10
V_{LED} (V)	28.06	22.48

From Table 2, the current sharing error percentage ε can be calculated as follows:

$$\begin{aligned}\varepsilon &= \left|\frac{0.3512-\frac{1}{2}(0.3512+0.3531)}{\frac{1}{2}(0.3512+0.3534)}\right|\times 100\% \\ &= \left|\frac{0.3531-\frac{1}{2}(0.3512+0.3531)}{\frac{1}{2}(0.3512+0.3531)}\right|\times 100\% = 0.27\%\end{aligned} \tag{36}$$

From Table 3, the current sharing error percentage ε can be calculated ε as follows:

$$\begin{aligned}\varepsilon &= \left|\frac{0.0855-\frac{1}{2}(0.0855+0.0871)}{\frac{1}{2}(0.0855+0.0871)}\right|\times 100\% \\ &= \left|\frac{0.0871-\frac{1}{2}(0.0855+0.0871)}{\frac{1}{2}(0.0855+0.0871)}\right|\times 100\% = 0.93\%\end{aligned} \tag{37}$$

Figure 23 shows the curve of current sharing error percentage rate from 25% to 100% loads. From this figure, it can be seen that the current error is below 1% all over the load range. Since the smaller the load is, the larger the current sharing error percentage, the proposed circuit uses 25% load as a design point for designing the differential-mode transformer T_1.

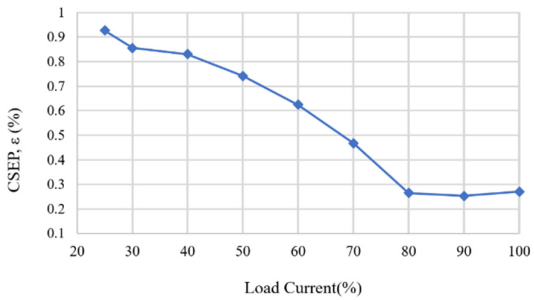

Figure 23. Current sharing error percentage ε from 25% to 100% loads.

 doi:10.20944/preprints202504.2363.v1

5.4. Efficiency Measurement

First, a digital meter is used to measure the input voltage, input current, and the output voltage and current of each LED string to obtain the input power and output power. Finally, the results are plotted to show the efficiency curve of the actual circuit. Figure 24 displays the efficiency curve efficiency versus load current.

From Figure 24, it can be seen that the efficiency is about above 93.6% over all the load range, the maximum efficiency is about 96.4% at 50% load, and the efficiency is about 94.4% at 100% load.

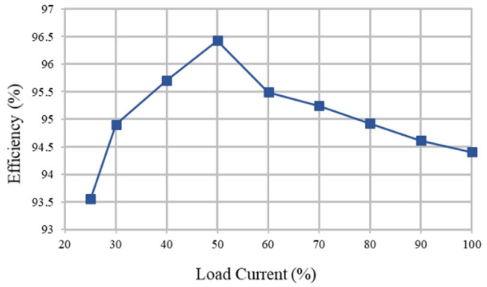

Figure 24. Curve of efficiency versus load current.

5.5. Switching Frequency Measurement

Figure 25 shows the curve of switching frequency versus load current. The switching frequency is about 132kHz at 100% load, whereas the switching frequency is 277kHz at 25% load. Also, from Figure 5, when the load current is higher, the value of Q is larger, so the frequency variation range is smaller; on the contrary, when the load current decreases, the frequency variation range is larger.

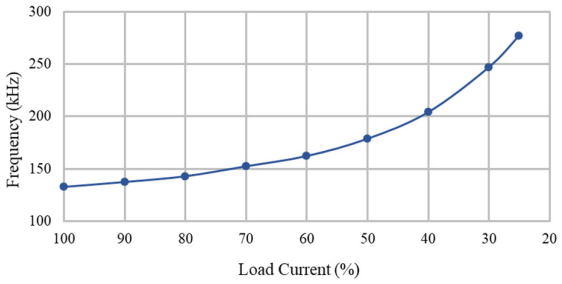

Figure 25. Curve of switching frequency versus load current.

6. Literature Comparison

Table 4 compares several items of components used in current equalization between the existing and proposed circuits, containing: (1) the number of LED strings; (2) the number of diodes required for four LED strings; (3) the wide adjustable load range; (4) the current equalization method; (5) the number of transformers required for four LED strings; (6) the soft switching; and (7) the extension of the number of LED strings.

Literatures [12,13] with differential-mode transformer equalization circuit, need to use a larger number of diodes to provide differential-mode transformer demagnetization path, and to ensure that this transformer can be completely demagnetized, the switching duty cycle has an upper limit, resulting in the ability to regulate the load being limited. The H-bridge circuit structure proposed in [24] reduces the number of demagnetizing diodes used in [12,13] and improves the load regulation. Literature [14] proposes to achieve current equalization of LED strings by connecting multiple isolation transformers in series, and the current equalization error is mainly determined by the magnitude of the magnetizing inductance of the isolation transformers, which also affects the load regulation capability of the resonant circuit. Therefore, a buck circuit is added in the front stage of

 doi:10.20944/preprints202504.2363.v1

the proposed circuit to change the duty cycle of the buck circuit, and the resonant circuit in the back stage adopts the fixed frequency operation to regulate the load current. In addition, in this current equalization method, it will lead to a relatively poor extension of the number of LED strings.

Table 4. Comparison between the existing and proposed circuits.

	[12]	[13]	[21]	[14]	Proposed Circuit
Number of LED strings	4	4	4	4	4
Number of diodes for four LED strings	8	8	2	4	4
Wide adjustable load range	No	No	Yes	Yes	Yes
Current equalization method	Transformer	Transformer	Transformer	Transformer and Capacitor	Transformer
Number of transformers for four LED strings	3	3	3	2	3
Soft switching	No	No	No	ZVS	ZVS
Extension of the number of LED strings	Yes	Yes	Yes	No	Yes

7. Conclusions

In this study, a non-isolated series resonant ZVS LED driver with current equalization is presented. In this LED driver, a differential-mode transformer is used to balance the LED currents. Furthermore, the series resonant converter uses a controlled frequency modulation to vary the amount of energy transferred to the outputs as well as to realize the turn-on ZVS. In addition, only the current in one LED string needs to be sensed, while the current in the other LED string is automatically determined by the differential-mode transformer, thereby simplifying control. In particular, the relationship between the magnetizing inductance and the current sharing error percentage is derived and can be used to design the value of the magnetizing inductance. By the way, from the experimental results, the current sharing error percentage is 0.27% at 100% load, and the efficiency is above 93.6% for any loads, with a maximum efficiency of 96.4%.

Author Contributions: Conceptualization, K.-I.H. and J.-Y.L.; methodology, J.-Y.L. and K.-I.H.; software, J.-Y.L.; validation, J.-Y.L. and K.-I.H.; formal analysis, J.-Y.L. and K.-I.H.; investigation, J.-Y.L.; resources, K.-I.H.; data curation, J.-Y.L.; writing—original draft preparation, K.-I.H.; writing—review and editing, K.-I.H..; visualization, J.-Y.L; supervision, K.-I.H.; project administration, K.-I.H.; funding acquisition, K.-I.H. All authors have read and agreed to the published version of the manuscript.

Funding: This research was funded by the Ministry of Science and Technology, Taiwan, under Grant Number NSTC112-2221-E-027-015-MY2.

Data Availability Statement: No new data were created or analyzed in this study. Data sharing is not applicable to this article.

Conflicts of Interest: The authors declare no conflicts of interest.

 doi:10.20944/preprints202504.2363.v1

References

1. De Almeida, A.; B, Santos, B.; Paolo, B. Quicheron, M. Solid state lighting review–Potential and challenges in Europe. *Renewable and Sustainable Energy Reviews*, **2014**, 34, 30-48.
2. Carraro, G. Solving high-voltage off-line HB-LED constant current control circuit issues. *APEC 07 - Twenty-Second Annual IEEE Applied Power Electronics Conference and Exposition*, **2007**, 1316-1318.
3. Burgyan, L.; Prinz, F. High efficiency LED driver. U.S. Patent 6690146B2, **2014**.
4. Hu, Y.; Jovanovic, M.M. LED driver with self-adaptive drive voltage. *IEEE Transactions on Power Electronics,* **2008**, 23, 3116-3125.
5. Qu, X.; Wong S.-C.; Tse, C.K. Noncascading structure for electronic ballast design for multiple LED lamps with independent brightness control. *IEEE Transactions on Power Electronics,* **2010**, 25, 331-340.
6. Hu, Q.; Zane, R. LED driver circuit with series-input-connected converter cells operating in continuous conduction mode. *IEEE Transactions on Power Electronics,* **2010**, 25, 574-582.
7. Kim, H.-C.; Yoon, C.S.; Jeong, D.-K.; Kim, J. A single-inductor, multiple-channel current-balancing LED driver for display backlight applications. *IEEE Transactions on Industry Applications,* **2014**, 50, 4077-4081.
8. Qu, X.; Wong, S.-C.; Tse, C.K. A current balancing scheme with high luminous efficiency for high power LED lighting," *IECON 2013 - 39th Annual Conference of the IEEE Industrial Electronics Society*, **2013**,169-174.
9. Doshi, M.; Zane, R. Digital architecture for driving large LED arrays with dynamic bus voltage regulation and phase shifted PWM. *APEC 07 - Twenty-Second Annual IEEE Applied Power Electronics Conference and Exposition*, **2007**, 287-293.
10. Wang, J.; Zhang, J.; Huang, X.; Xu, L. A family of capacitive current balancing methods for multi-output LED drivers. *2011 Twenty-Sixth Annual IEEE Applied Power Electronics Conference and Exposition* (*APEC*), **2011**, 2040-2046.
11. Do, D.-T.; Cha, H.; Nguyen, B.L.-H.; Kim, H.-G. Two-channel interleaved buck LED driver using current-balancing capacitor," *IEEE Journal of Emerging and Selected Topics in Power Electronics,* **2018**, 6, 1306-1313.
12. Hwu, K.I.; Chou, S.-C. A simple current-balancing converter for LED lighting. *2009 Twenty-Fourth Annual IEEE Applied Power Electronics Conference and Exposition,* **2009**, 587-590.
13. Hwu, K.I.; Tu, W.C.; Hong, M.J. A dimmable LED driver based on current balancing transformer with magnetizing energy recycling considered. *Journal of Display Technology,* **2014**, 10, 388-395.
14. Chen, X.; Huang, D.; Li, Q.; Lee, F.C. Multichannel LED driver with LCC resonant converter. *IEEE Journal of Emerging and Selected Topics in Power Electronics*, **2015**, 3, 589-598.
15. Zhang, Xiangjun; Cai, Hongye; Guan, Yueshi; Han, Shouheng; Wang, Yijie; Dalla Costa, Marco A.; Alonso, Jose Marcos; Xu, Dianguo. A soft-switching transformer-less step-down converter based on resonant current balance module," *IEEE Transactions on Power Electronics*, **2021**, 7, 8206-8218.
16. Zhang, X.; Cai, Sun, H.L.; Liu, H.; Wang, Y.; Xu, D. A two-channel LED driver with automatic current balance and soft-switching. *2020 IEEE 9th International Power Electronics and Motion Control Conference (IPEMC2020-ECCE Asia)*, **2020**, 2594-2598.
17. Jiang, W.-Z.; Hwu, K.-I.; Yau, Y.-T.; Chen, H.-H. Two-channel LLC resonant LED driver based on current sharing capacitor. *2021 IEEE International Future Energy Electronics Conference (IEFFC)*, **2021**, 1-7.
18. Molavi, N.; Farzanehfard, H. A nonisolated wide-range resonant converter for LED driver applications. *IEEE Transactions on Industrial Electronics,* **2023**, 70, 8939-8946.
19. Hsieh, Y.-C.; Cheng, H.-L.; Chang, E.-C.; Huang, W.-D. A soft-switching interleaved buck–boost LED driver with coupled inductor. *IEEE Transactions on Power Electronics*, **2022**, 37, 577-587.
20. Lee, S.-W.; Choe, H.-J.; Yun, J.-J. Performance improvement of a boost LED driver with high voltage gain for edge-lit LED backlights. *IEEE Transactions on Circuits and Systems II: Express Briefs*, **2018**, 65, 481-485.
21. Jiang, W.-Z.; Hwu, K.-I. A dimmable LED driver based on H-bridge and differential-mode transformer. *2018 7th International Symposium on Next Generation Electronics (ISNE)*, **2018**, 1-3.